

## How the infrared radiation affects the film formation process from latexes?

O. Yargi,<sup>1</sup> A. Gelir,<sup>2</sup> M. Ozdogan,<sup>1</sup> C. Nuhoglu,<sup>1</sup> A. Elaissari<sup>3</sup>

<sup>1</sup>Department of Physics, Yildiz Technical University, Esenler 34210, Istanbul, Turkey

<sup>2</sup>Department of Physics, Istanbul Technical University, Maslak 34469, Istanbul, Turkey

<sup>3</sup>Lagep Laboratory, Claude Bernard University, 69622 Lyon-1, France

Correspondence to: O.Yargi (E-mail: oyargi@yildiz.edu.tr)

**ABSTRACT:** In this study, the effect of the infrared radiative heating (IRH) was investigated on the film formation from composites of polystyrene (PS) latex particles and poly vinyl alcohol (PVA). The films were prepared as a pure PS and a mixture of PS and PVA particles at equal compositions at room temperature and they were annealed at elevated temperatures above the glass transition temperature ( $T_g$ ) of PS for 10 min by using IRH technique. Identical experiments were performed by using standard convectional heating technique in oven as comparison. It was shown that the activation energy for the film formation from PS latex particles decreased considerably in IRH annealing technique. Photon transmission (PT) and steady state fluorescence (SSF) techniques were used to monitor the film formation process at each sintering step. Minimum film formation temperature,  $T_o$ , and healing temperature,  $T_h$ , were determined by the data obtained from the SSF and the PT measurements for each heating processes. The film formation was modeled as a void closure and as an interdiffusion stage below and above  $T_h$ , respectively. Scanning electron microscopy (SEM) was used to examine the variation in morphological structure of annealed composite films. It was observed that IRH heating causes more homogenous and more flat film surface than films annealed in the oven. © 2015 Wiley Periodicals, Inc. *J. Appl. Polym. Sci.* **2016**, *133*, 43289.

**KEYWORDS:** films; glass transition; polystyrene; spectroscopy

Received 12 October 2015; accepted 1 December 2015

DOI: 10.1002/app.43289

### INTRODUCTION

Nowadays, radiation from infrared sources has gained attention especially for heating. IR radiation has been applied to dry foods<sup>1</sup> and waterborne polymers.<sup>2,3</sup> The drying time of aqueous solutions of poly(vinyl alcohol) was reduced from 120 min, which is for convective drying, to only 15 min for combined convective and IR radiative drying.<sup>2</sup> IR heating has some advantages comparing with the heating with convection.<sup>4</sup> First, the slow rate of heat transfer through air in convective heating leads to long heat-up times in convection ovens. Using infrared emitters, it is possible to heat surfaces rapidly because of high transfer of energy and minimize the conduction losses. Second, the combustion products, recirculation of dust, etc. make convective heating unsuitable for “clean” applications. Since the IR heating does not produce any combustion and does not need any recirculation of air, it is clearer than the convectional heating. Third, the time to reach the operating temperature for the convection ovens lasts from 30 min to 2 h depending on the size of the convection oven which means that the oven must be turned on to reach the required temperature much before the experiment. But for infrared emitter, this time is very short because it can

be switched on and off within very short time intervals and by adjusting the electrical voltage applied on the emitter, it can reach the operating temperature in a very short time. Fourth, in convective heating in an oven, heat diffuses from the film surface and the time for homogeneous distribution of temperature through the film directly depends on this heat diffusion. However, in infrared radiative heating (IRH) process, the electromagnetic energy can be focused directly on the film which leads to a drastic decrease in time to reach a homogeneous distribution of temperature through the film.

Latex films are generally formed by coalescence of submicrometer polymer particles in the form of a colloidal dispersion, usually in water. Aqueous dispersions of colloid particles with  $T_g$  below the drying temperature known as low-T latex (soft latex in which the particles are of submicrometer size). To understand the mechanism of homogeneous film formation from latex particles is quite important for enhancing the quality of coatings. Traditionally, the film formation process of polymer latex is considered in terms of three sequential steps: (i) Colloid concentration increases as water evaporates, a uniform shrinkage of the interparticle distance occurs, and the voids are

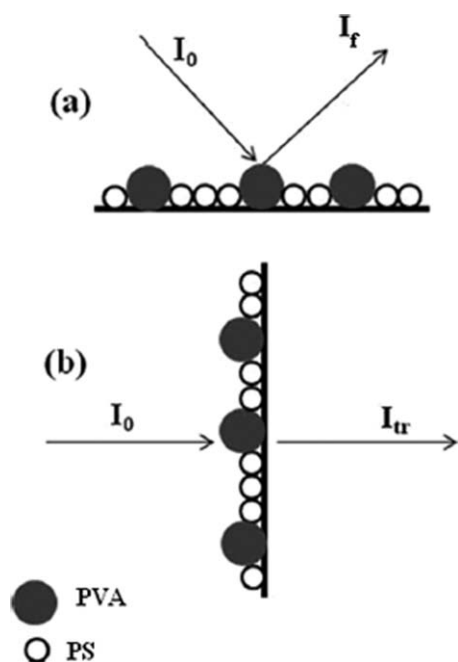


**Figure 1.** Schematic illustration of the sample position for (a) fluorescence and (b) UV transmittance measurements.

gradually filled by particle sliding until a dense packing of spheres is obtained. (ii) Deformation of the particles and close contact between the particles if their  $T_g$  is less than or close to the drying temperature (soft or low  $T_g$  latex). Latex with a  $T_g$  above the drying temperature (hard or high  $T_g$  latex) stays undeformed at this stage. Annealing of a hard latex system above the minimum film formation temperature, deformation of particles first leads to void closure<sup>5,6</sup> and then after the voids disappear, diffusion across particle–particle boundaries starts, i.e., the mechanical properties of hard latex films evolve during annealing. Particles are deformed to polyhedrons where the deformation is driven by the combination of surface and osmotic forces until all solvent has evaporated and all voids have disappeared. (iii) Coalescence of the deformed particles to form a homogeneous film<sup>6</sup> where macromolecules belonging to different particles mix by interdiffusion.<sup>7,8</sup> This understanding of latex film formation can now be exploited to underpin the processing of new types of coatings and adhesives. The blending of latex particles and inorganic nanoparticles provides a facile means of ensuring dispersion at the nanometer scale in composite coatings.

Several experimental techniques were used to observe latex film formation such as electron<sup>9</sup> and atomic force microscopies,<sup>10</sup> neutron scattering,<sup>11</sup> nonradiative energy transfer conjunction with time resolved,<sup>12</sup> and steady state fluorescence.<sup>13</sup> Light has been used to monitor the film formation for a long time. Ellipsometry,<sup>14</sup> photon transmission (PT),<sup>15–17</sup> and reflection<sup>18</sup> techniques have been elaborated for latex film formation processes. Scanning<sup>19</sup> and transmission<sup>20</sup> electron microscopes have been commonly used techniques to characterize the latex systems.

Previously, an electrically conducting polymer (polypyrrole) has been applied as a thermal transducer to raise the temperature of

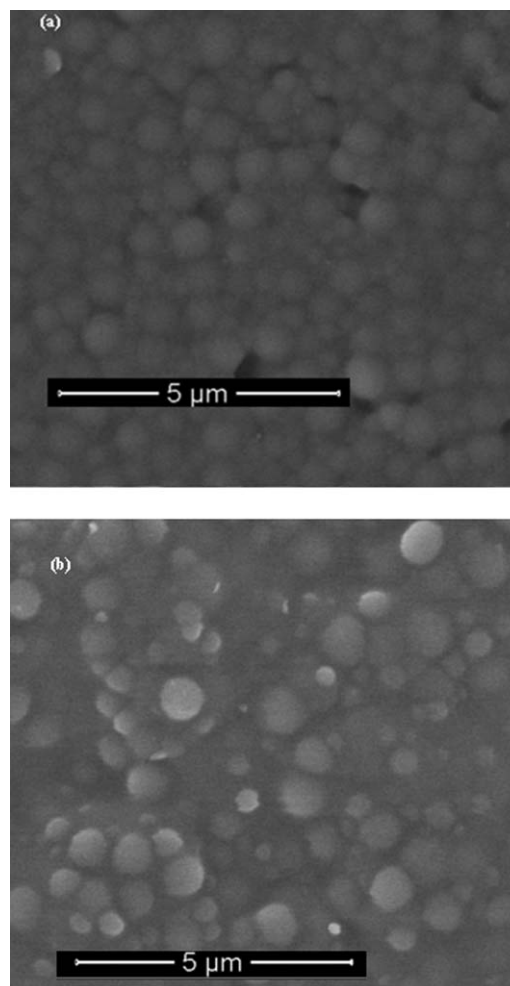


**Figure 2.** SEM image of (a) pure PS and (b) PS/PVA (50 wt %) composite latex films.

microspheres<sup>21</sup> and hot-melt adhesives<sup>22</sup> under NIR (Near IR) radiation. Nowadays, (polyaniline and poly (3,4-ethylenedioxythiophene) [PEDOT])<sup>23</sup> have been shown to be effective at enhancing IR heating because of their strong absorption characteristics.

In this work, we investigated the film formation behavior of pure Polystyrene (PS) and PS and Poly Vinyl Alcohol, (PS/PVA) composites depending on two different heating processes, IRH and convective heating using PT and fluorescence techniques steady state fluorescence (SSF). PS was chosen as main constituent because of being easily processes, solubility in a broad range

**Table I.** Experimentally Obtained Void Closure ( $\Delta H$ ) and Interdiffusion Energies ( $\Delta E$ ) NC: Cannot be calculated

kcal/mol	PS- $I_{tr}$	PS/PVA- $I_{tr}$	PS- $I_f$	PS/PVA- $I_f$
$\Delta H$ -OVEN	2.30	0.53	0.97	0.62
$\Delta E$ -OVEN	2.78	1.01	23.1	18.0
$\Delta H$ -IR	0.67	NC	0.72	NC
$\Delta E$ -IR	1.08	NC	37.4	NC

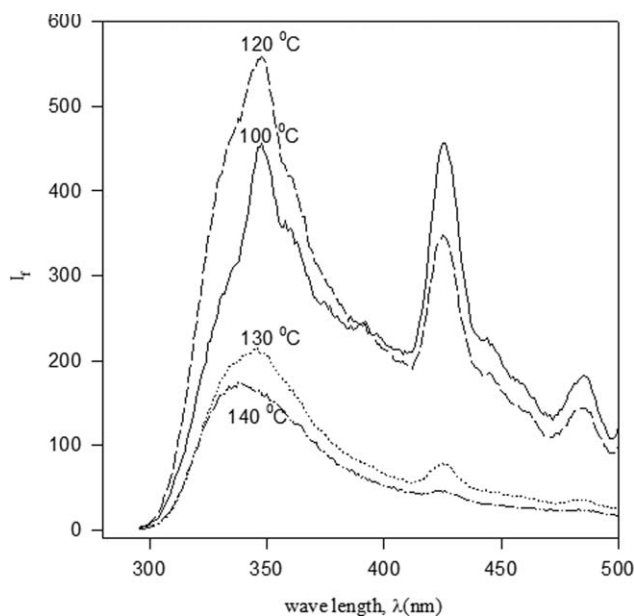


**Figure 3.** The fluorescence spectra of the pure PS latex films at different temperatures.

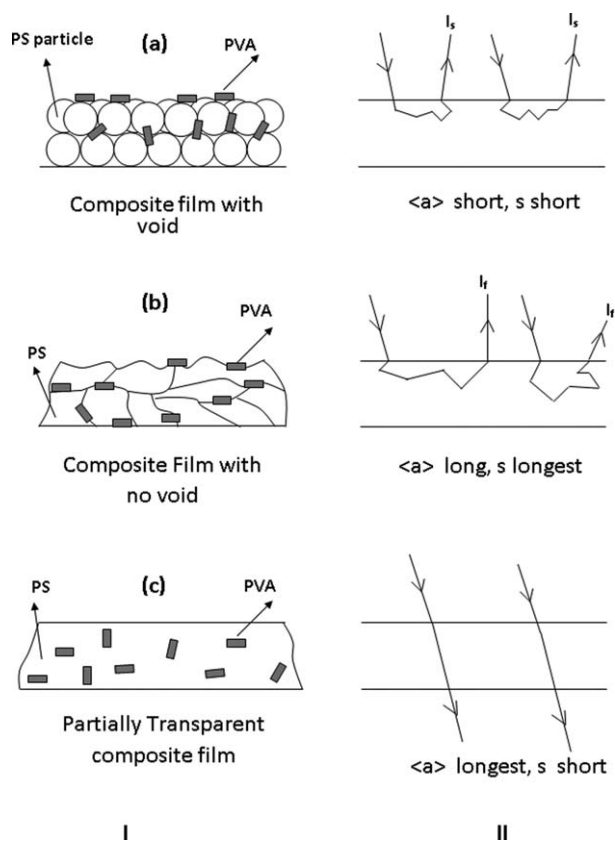


**Figure 4.** Schematic illustration of the stages of the latex film formation and the path of the light inside the film at each stage. (a) The initial stage of the film formation. Film mostly has voids inside. (b) The voids inside the film are disappeared upon annealing. (c) The final stage of the film formation. Here the partially transparent film is obtained because of the interdiffusion of the polymers through the boundaries.

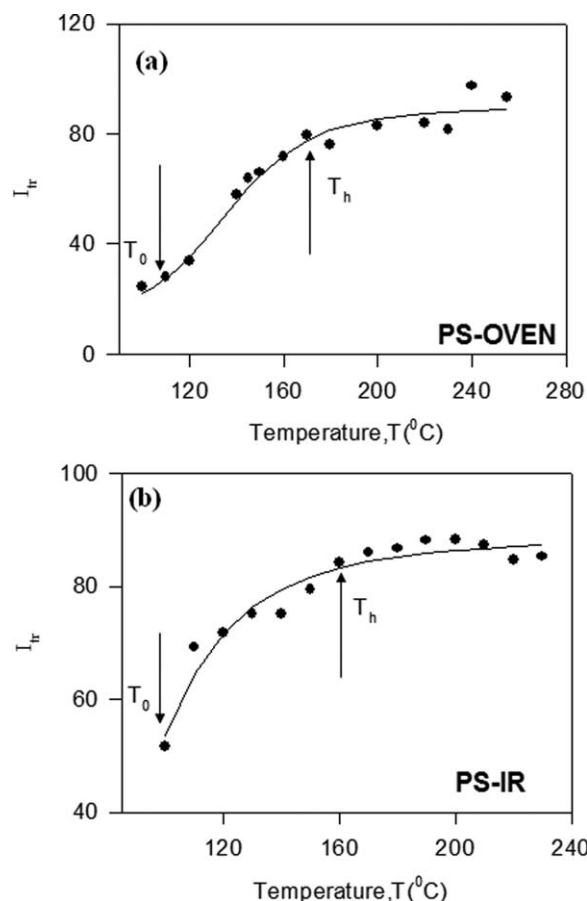


**Figure 5.** Transmitted light intensity ( $I_{tr}$ ) versus temperature for the pure PS latex film annealed by (a) conventional heating in the oven and (b) IRH.

of solvents and its clarity which allows dispersion of PVA to be optically observable at the micron scale. After each annealing step, the transmitted light intensity,  $I_{tr}$ , and the fluorescence intensity,  $I_f$ , was monitored to observe the film formation in the two separate heating conditions. The increase in  $I_{tr}$  and  $I_f$  was explained by void closure up to healing temperature,  $T_h$ , and above  $T_h$  it was explained by the interdiffusion processes for both IRH and convective heating.

## EXPERIMENTAL

### Materials

Fluorescent PS latexes were prepared via a surfactant free emulsion polymerization process of styrene monomer (99% pure from Alfa Asea) using (Potassium persulphate) KPS as initiator. The fluorescent latexes were prepared by adding fluorescent monomer dimethacrylate (PolyFluor™ 511 from Polysciences) in pre-polymer solution. The water-soluble radical initiator KPS was dissolved in water and added when the polymerization temperature reached 90°C. In all polymerizations, deionized water was used.

Commercially available Polyvinyl alcohol, PVA (Boysan, Turkey, include Acetic acid ethenyl, ester, polymer with ethanol, 92–100%, powder form and water soluble, white color, melting point is 220–240°C, PH is 4.5–6.5) was used as supplied in white powder form. A stock solution of PVA was prepared by

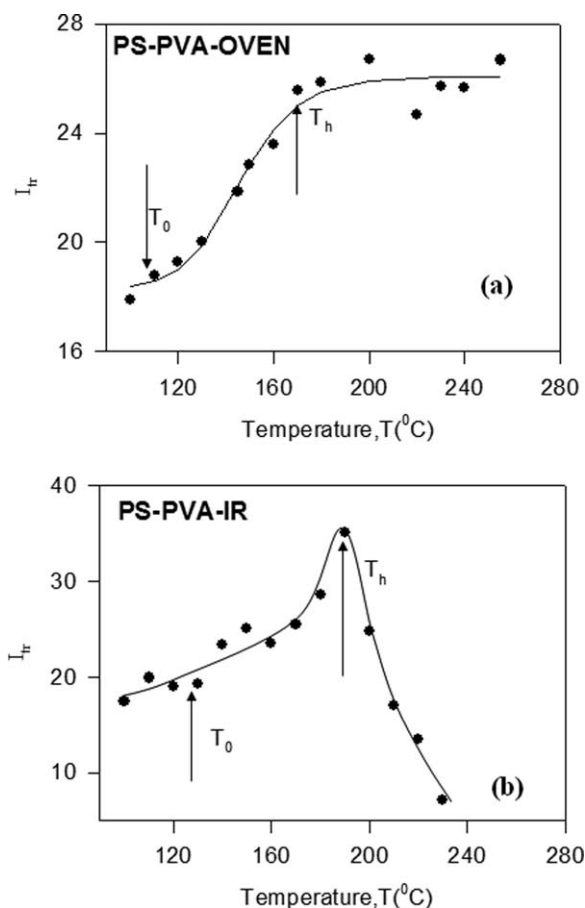


**Figure 6.** Transmitted light intensity ( $I_{tr}$ ) versus temperature for the PS/PVA (50 wt %) composite latex film annealed by (a) conventional heating in the oven and (b) by IRH.

following the manufacturers regulations: PVA were dispersed in deionized (DI) water with in the proportions of 0.01 g PVA; 1 mL DI water by bath sonication for 3 h. PVA is a good stabilizing for dispersions enabling preparation of PS composites from dispersions of PVA in PS solution.

#### Film Preparation

Two different films with (0 wt % PVA and 50 wt % PS/PVA contents) and two sets were prepared from the dispersion of PS/PVA composites by placing the same number of drops on a glass plates with the size of  $0.8 \times 2.5 \text{ cm}^2$  and allowing the water to evaporate. One set was prepared for the convective heating and the other set was prepared for IRH. Then the samples were separately annealed above  $T_g$  of PS,  $105^\circ\text{C}$ , for 10 min at temperatures ranging from 100 to  $270^\circ\text{C}$  in both oven and under IR lamb. The temperature was maintained within  $\pm 2^\circ\text{C}$  during annealing for oven and  $\pm 1^\circ\text{C}$  for IRH.

After annealing, each sample was placed in the solid surface accessory of a Varian Carry Eclipse fluorescence spectrometer. Fluoroprobe, dimethacrylate, in the film was excited at 255 nm and the maximum of the fluorescence emission was observed at 347 nm. All measurements were carried out in the front-face position at room temperature. Slit widths were kept at 8 nm

during all SSF measurements. The sample position, the incident light,  $I_0$ , and the emitted light,  $I_f$  are shown in Figure 1(a), where it is seen that  $I_f$  is collected at right angle with respect to the incident light. PT measurements were performed by using UV-Visible spectrometer, Perkin Elmer Lambda 35. The transmittances of the films were detected at 500 nm. A glass plate was used as a standard for all transmittance experiments and measurements were carried out at room temperature after each annealing processes. The sample position and the transmitted light,  $I_{tr}$ , are presented in Figure 1(b). Scanning Electron Microscopy (SEM) images of pure PS and PS/PVA composites were obtained by FEI-Quanta FEG 250 scanning probe microscopy.

#### Calculation of the Activation Energies

The activation energies for the void closure process are calculated by using the following equation<sup>24,25</sup>:

$$I(T) = S(t) \exp\left(-\frac{3\Delta H}{kT}\right) \quad (1)$$

where  $S(t) = (yt/2AC)^3$ ,  $k$  is the Boltzmann's constant,  $\Delta H$  is the void closure energy, and  $I$  is the either transmittance at

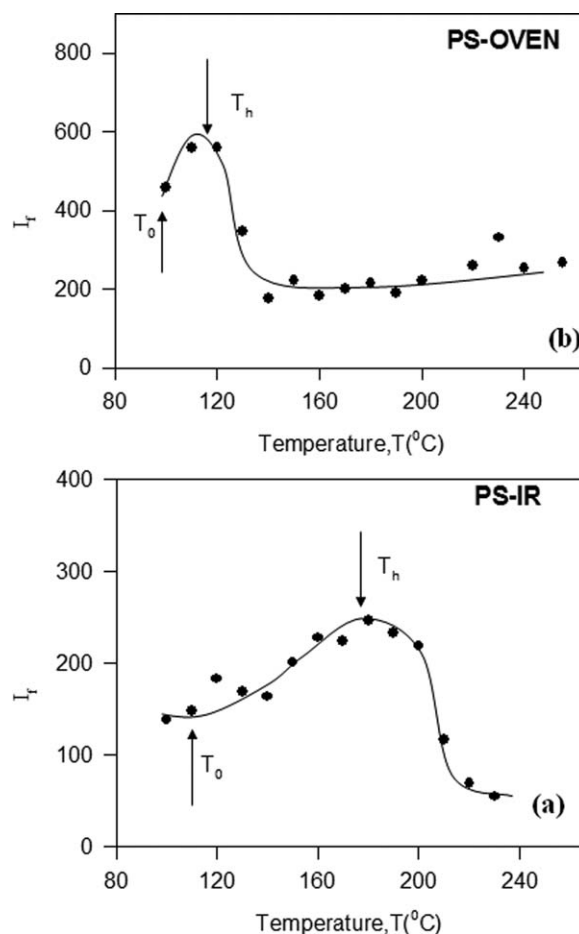


**Figure 7.** Fluorescence intensity ( $I_f$ ) at 357 nm versus temperature for the pure PS latex film annealed by (a) conventional heating in the oven and (b) by IRH. The excitation wavelength is 255 nm.

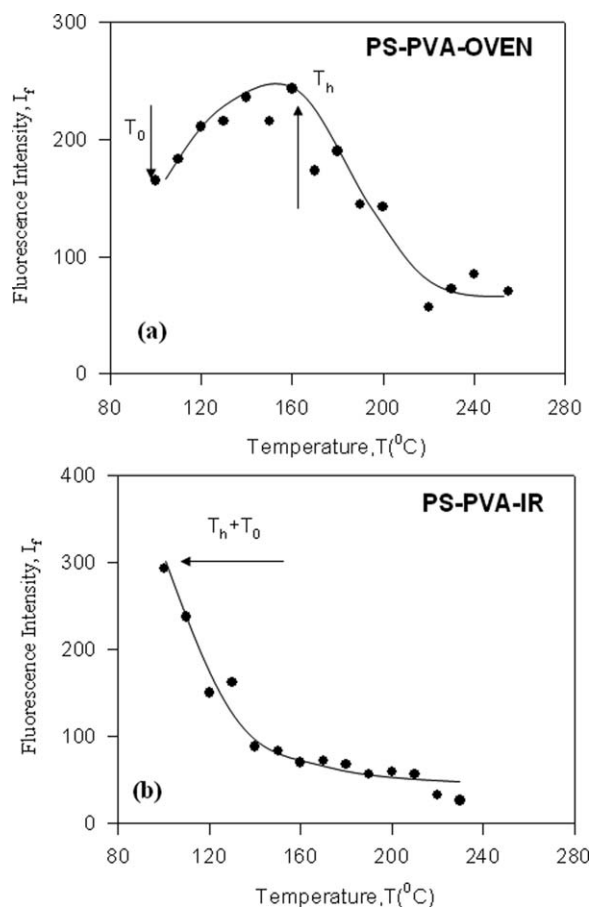


**Figure 8.** Fluorescence intensity ( $I_f$ ) at 357 nm versus temperature for the PS/PVA (50 wt %) composite latex film annealed by (a) conventional heating in the oven and (b) by IRH. The excitation wavelength is 255 nm.

500 nm or fluorescence intensity at 347 nm. For a given time the logarithmic form of eq. (1) can be written as follows

$$\ln I_f(T) = \ln S(t) - \left( \frac{3\Delta H}{k_B T} \right) \quad (2)$$

By using the least square fitting, the void closure energy can be calculated by using eq. (2) for the latex films.

The activation energies for the interdiffusion process are calculated by using the following equation:

$$I(T)/I(\infty) = A \exp(-\Delta E/2kT) \quad (3)$$

where  $k$  is the Boltzmann's constant,  $\Delta E$  is the interdiffusion energy, and  $I$  is the either transmittance at 500 nm or fluorescence intensity at 347 nm. Similar procedure with the calculation of the void closure energies is used to calculate the interdiffusion energy.

The activation energies for the PS and PS/PVA films annealed by the convective heating in the oven and IRH monitored by UV transmittance and fluorescence techniques were given in Table I.

Since the theoretical models which describe the latex film formation are discussed in literature in detail,<sup>24,25</sup> the information about these models was not given in this manuscript.

## RESULTS AND DISCUSSION

The emission spectra of pure PS latex films annealed for 10 min at various temperatures are shown in Figure 3, where it is seen that  $I_f$  first increases and then decreases upon annealing. The behavior of  $I_f$  can be explained with the schematic picture given in Figure 4. In Figure 4(a), at the early stages of the film formation, the composite film possesses many voids which results in short mean free,  $\langle a \rangle$ , and optical,  $s$ , paths of photons. At this stage most of the light is scattered which yields low  $I_f$ . Figure 4(b) represents a film in which interparticle voids disappear because of the annealing. The mean free path and the optical path are the longest for this case and  $I_f$  reaches its maximum value because of the increasing efficiency of the excitation because of the long  $s$ . Finally, as seen in Figure 4(c), a partially transparent film with longest  $\langle a \rangle$  but shorter  $s$  values was formed. Since the optical path is very small compared with the previous condition, the excitation efficiency decreases considerably resulting in low  $I_f$  intensity.

Transmitted light intensity,  $I_{tr}$ , versus annealing temperatures is plotted in Figures 5 and 6 for the PS films without and with PVA (%50 PS, %50 PVA), respectively.  $I_{tr}$  first starts to increase after a certain onset temperature, called the minimum film formation temperature  $T_o$ , and then reaches a maximum at the healing temperature,  $T_h$ , which is the transition temperature

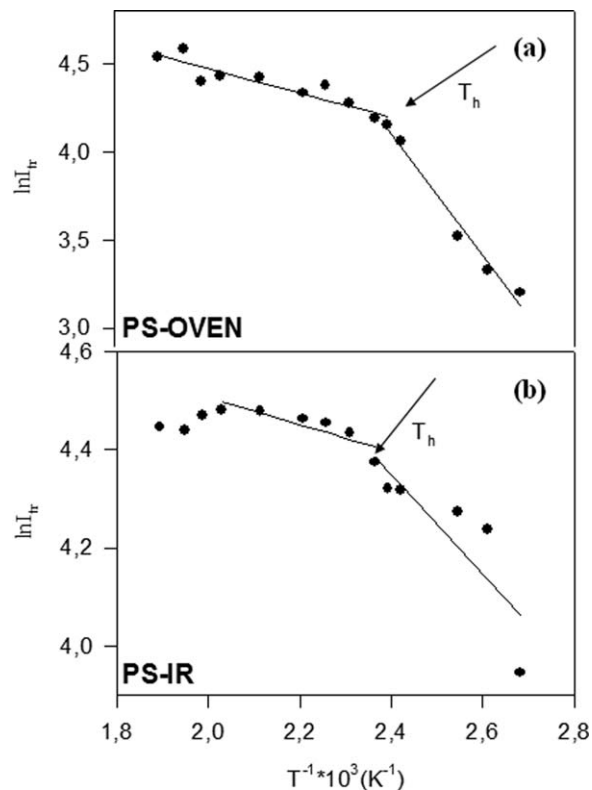


**Figure 9.** Logarithmic plots of  $I_{tr}$  data vs. inverse of annealing temperatures ( $T^{-1}$ ) for the pure PS latex films annealed for 10 min in (a) oven and (b) IRH. Data are fitted to eqs. (2) and (3) to produce  $\Delta H_{tr}$  (right slopes) and left slope of the linear relations produces  $\Delta E_b$  values, respectively which are listed in Table I.

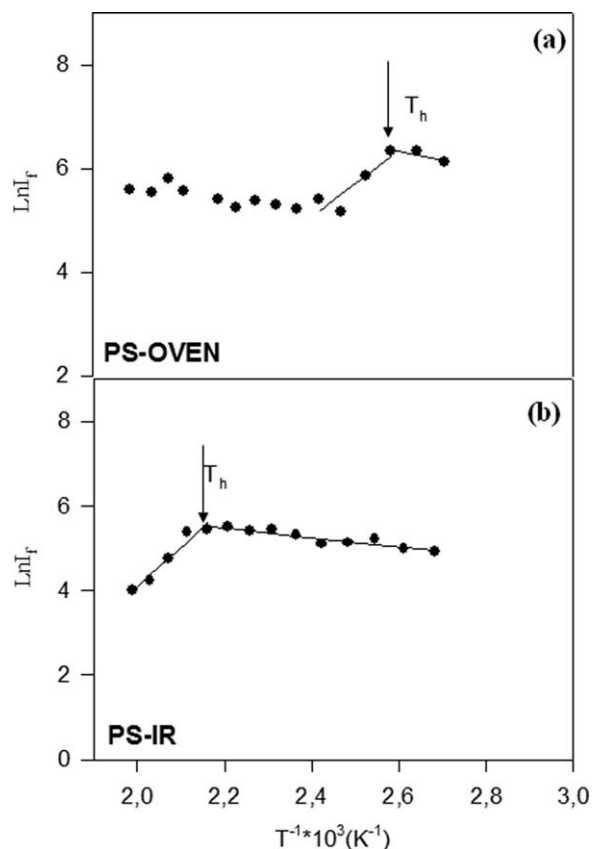


**Figure 10.** Logarithmic plots of  $I_f$  data vs. inverse of annealing temperatures ( $T^{-1}$ ) for the pure PS latex films annealed for 10 min in (a) oven and (b) IRH. Data are fitted to eqs. (2) and (3) to produce  $\Delta H_p$  (right slopes) and left slope of the linear relations produces  $\Delta E_b$  values, respectively which are listed in Table I.

from void closure to interdiffusion process. The increase in  $I_{tr}$  above  $T_o$  can be explained by the evaluation of the transparency of the PS and PS/PVA latex films upon annealing. Most probably, increased  $I_{tr}$  corresponds to the void closure process; i.e., polymer starts to flow upon annealing and voids between particles can be filled. After  $T_h$  since the motion of the polymers through the boundaries during the interdiffusion process does not change the average optical properties of the latex films, the increase rate of the transmittance is very small.<sup>24,25</sup> Just for the PS/PVA latex film annealed by IRH technique;  $I_{tr}$  decreases after reaching maximum as seen in Figure 6(b). This point will be discussed in the following paragraphs.

For pure PS films, both  $T_o$  and  $T_h$  values are close to each other in both infrared and convective heating techniques as seen in Figure 5. But the rate of increase and the initial value of the transmittance are higher for the film annealed by IRH [Figure 5(b)]. Also the void closure ( $\Delta H$ ) – interdiffusion ( $\Delta E$ ) energies obtained from Figure 9 are 2.30–2.78 kcal/mole and 0.67–1.08 kcal/mole for PS films annealed by the convective heating in the oven and IRH, respectively, as given in Table I. These results clearly indicate that less energy is required for the void closure and interdiffusion processes for the pure PS latex films when IR heating is used for the film formation.

The transmittance variations with respect to the annealing temperature for the PS/PVA composite latex films annealed by the convective heating in the oven and IRH are shown in Figure 6. The void closure and the interdiffusion processes are clearly observable for the composite films annealed in the oven and the required energies for these processes are calculated as 0.53 and 1.01 kcal/mole, respectively (see Figure 11). Here it has to be noted that the measured activation and interdiffusion energies for viscous flow were found to be different in different techniques (Fluorescence and PT) Since PS particles have fluorescence characteristic, it is believed in that values using fluorescence spectrometer are more realistic to interpret the viscous flow. It is also seen that  $\Delta E$  values are higher than  $\Delta H$  values for both PS and PS/PVA composites. Since PS particles can screen the motion of polymer chain across the junction, then, a single chain needs more energy to overcome this difficulty. Therefore a single chain needs more energy to execute diffusion across the polymer–polymer interface, than bulk polymer needs to accomplish the viscous flow process. Another interesting point is that, the obtained void closure and interdiffusion energies from PS/PVA composites is less than PS particles for the two techniques as seen in Table I. This result shows that addition of the PVA particles makes easier film formation processes. Probably, when PVA particles heated around the  $T_g$  value starts to fill the voids

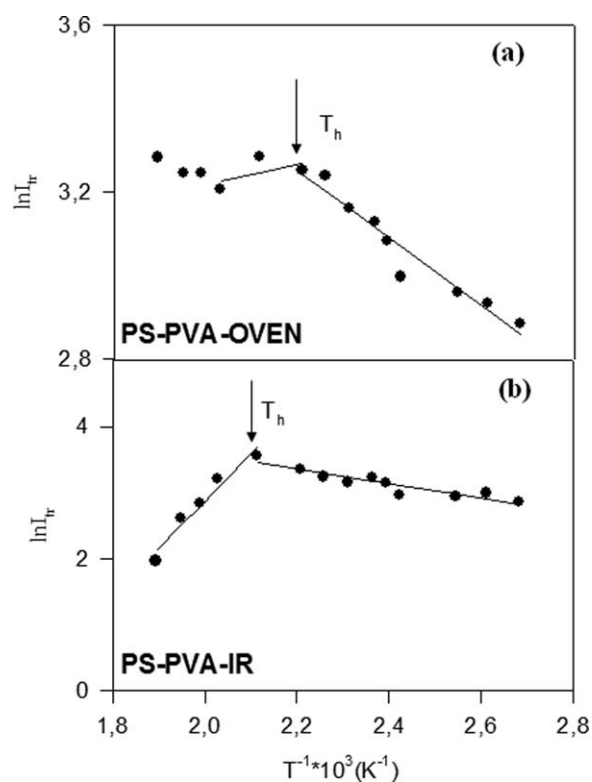


**Figure 11.** Logarithmic plots of  $I_{tr}$  data vs. inverse of annealing temperatures ( $T^{-1}$ ) for the PS/PVA composite films annealed for 10 min in (a) oven. Data are fitted to eqs. (2) and (3) to produce  $\Delta H_{tr}$  (right slopes) and left slope of the linear relations produces  $\Delta E_b$  values, respectively which are listed in Table I. and (b) Logarithmic plots of  $I_{tr}$  data vs. inverse of annealing temperatures ( $T^{-1}$ ) for the PS/PVA composite films annealed for 10 min by IRH.

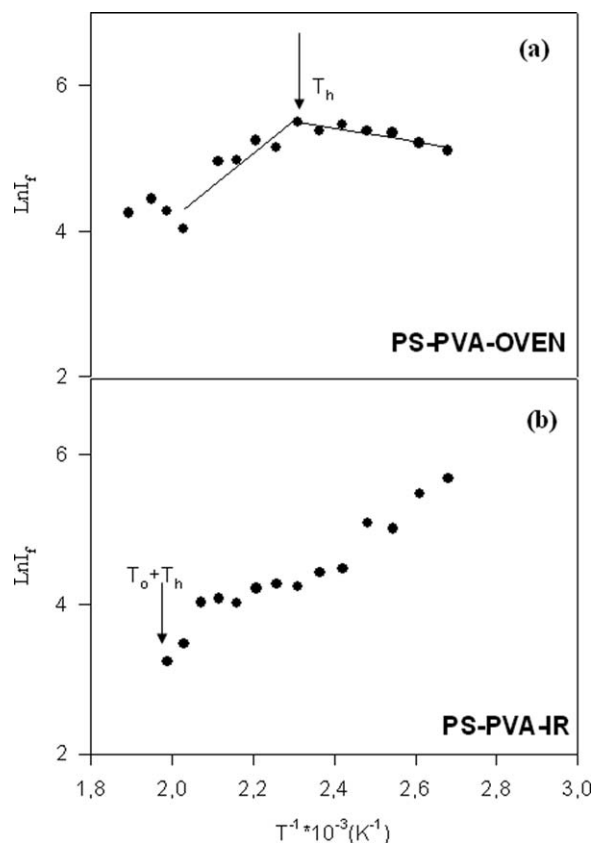


**Figure 12.** Logarithmic plots of  $I_f$  data vs. inverse of annealing temperatures ( $T^{-1}$ ) for the PS/PVA composite films annealed for 10 min in (a) oven. Data are fitted to eqs. (2) and (3) to produce  $\Delta H_f$  (right slopes) and left slope of the linear relations produces  $\Delta E_b$  values, respectively which are listed in Table I. (b) Logarithmic plots of  $I_f$  data vs. inverse of annealing temperatures ( $T^{-1}$ ) for the PS/PVA composite films annealed for 10 min by IRH.

between the PS particles and decreases the aggregation in two polymer system and causes being more homogenous film structure. Figure 14 is also support this finding that film structure of PS/PVA composites are seen smoother than pure PS film after applying IRH. In other words, film formation processes is already completed for IRH at 160°C, while pure PS particles need higher temperatures using oven. For the PS/PVA film annealed by IRH, different situation was observed: the transmittance decreased abruptly after reaching maximum value as seen in Figure 6(b). This decrease in the transmittance is probably because of the physical deformation of the film. Because some dark spots were observed on the surface of the PS/PVA film annealed by IRH after a certain temperature. Before the maximum  $I_{tr}$ , probably the void closure and the interdiffusion processes occur very fast and nearly simultaneously. So it cannot be possible to distinguish these processes during the film formation for the PS/PVA composite film annealed by IRH. This prediction is supported by the SEM micrographs given in Figures 13 and 14. Here it is clearly seen that the films annealed by IR heating are more homogeneous than those annealed in the oven which indicates that the film formation is completed in shorter times for the IR heating system.

The changes in the fluorescence emission intensity at 347 nm with respect to temperature for the pure PS latex films annealed by convective heating in the oven and IRH are given in Figure 7. The overall behavior is in accordance with the stages of the film formation given in Figure 4. Until the end of the void closure processes, the optical path of the light inside the film increases which results in increasing excitation efficiency and thus increasing fluorescence emission intensity. On the other hand, after the void closure stage is completed, the optical path starts to decrease which means that the fluorescence emission intensity also decreases. The void closure energies calculated fluorescence data obtained from Figure 10 are 0.97 and 0.72 kcal/mole for the PS films annealed in the oven and IRH, respectively, as given in Table I. Again the required energy for the void closure process is smaller for the IRH system than the oven which is in accordance with the results of the transmittance measurements.

Another interesting point in Figure 7 is that the temperature behaviors of the fluorescence intensity with respect to temperature for films annealed by the convective heating in the oven and IRH are different. The fluorescence intensity of the film annealed by IRH is smaller than that for the film annealed in

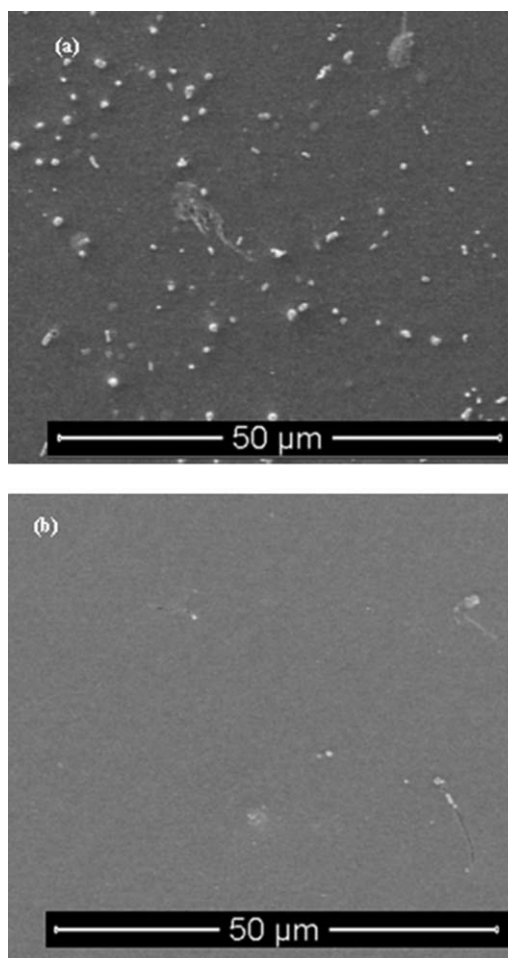


**Figure 13.** (a) SEM images of the pure PS latex film annealed in the oven at 250°C, (b) SEM images of pure PS latex film annealed by IRH at 250°C.

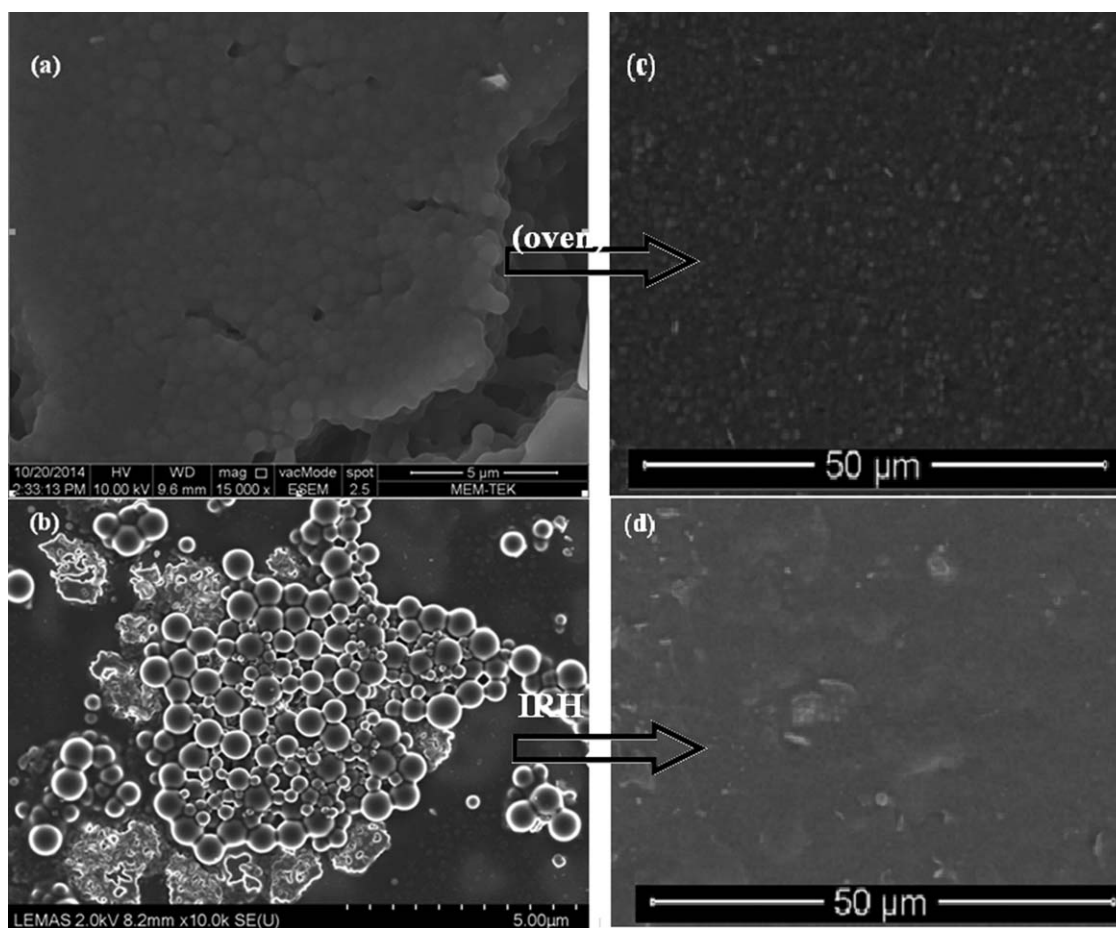


**Figure 14.** (a) SEM images of pure PS latex film annealed in the oven at 100°C. (b) SEM images of the 50 wt % PS in PS/PVA composite latex film annealed in the oven at 100°C (c) SEM images of the pure PS latex film annealed in the oven at 160°C, (d) SEM images of 50 wt % PS in PS/PVA latex film annealed by IRH at 160°C.

the oven. This indicates that a more homogeneous film formation is obtained by IRH which is in accordance with the SEM images given in Figures 13 and 14. Since the film is more homogeneous, the change in the optical path,  $s$ , upon annealing is not so big when compared with the optical path change for the film annealed in the oven. This decreases the sensitivity of the fluorescence technique in the observation of the void closure process and the temperature for the void closure reaches higher values for the film annealed by IRH as seen in this figure.

The healing temperatures for the films annealed in the oven and IRH are different as seen in this figure; on the other hand these were close to each other in the transmittance measurements as mentioned above. The healing temperatures for the films annealed in the oven are completely different for different measurement techniques, around 160°C for transmittance and 110°C for fluorescence. But these temperatures are close to each other for the films annealed by IRH, about 160°C for both transmittance and fluorescence. This result clearly indicates that the film formation process by IR heating can be monitored by both transmittance and fluorescence techniques simultaneously.

The fluorescence emission intensity at 347 nm with respect to annealing temperature for the composites PS/PVA films annealed

by the convective heating in the oven and IRH are given in Figure 8. The behavior of the composite PS/PVA film annealed in the oven [Figure 8(a)] is similar to the pure PS film annealed in the oven [Figure 7(a)]. The fluorescence emission intensity first increases and then it decreases as explained in the previous paragraphs. But the behavior is different for the PS/PVA composite film annealed by IRH. Here the fluorescence emission intensity decreases for the whole process. This observation is in accordance with the results of the transmittance measurements given in Figure 6(b) where it was discussed that the IRH speeds up the film formation process which causes the void closure and the interdiffusion proceeds almost simultaneously. Therefore, for the composite film annealed by IRH the optical path and thus the fluorescence emission intensity decreases during the film formation process and this makes the monitoring of the film formation stages for the composite film annealed by IRH impossible. Only the void closure and the interdiffusion energies for the composite film annealed in the oven could be calculated as 0.62 and 18.00 kcal/mole, respectively as in Table I (see Figure 12). These energies are in accordance with the energies calculated from the transmittance measurements which clearly indicate that the energy for the motion of the polymers through the boundaries is much higher than the void closure energy.



## CONCLUSIONS

This study mainly focused on the effect of the IR heating on the film formation process of the pure PS and PS/PVA composite latex films. The following conclusions can be made as a result of the experiments performed in this study.

- i. The film formation stages of the pure PS latex films annealed by the convective heating in the oven and by IRH could be monitored by both transmittance and the fluorescence techniques. On the other hand, the film formation stages of the PS/PVA latex films annealed by the convective heating in the oven and by IRH could only be observed by the transmittance measurements.
- ii. When the IRH technique is used for the film formation of the pure PS latex films, the void closure and the interdiffusion activation energies decreases considerably as seen in Table I.
- iii. The latex films annealed by IRH are more homogeneous than the latex films annealed by the convective heating in the oven.
- iv. Finally it can be concluded that the IRH technique speeds up the film formation process for the latex films.

## ACKNOWLEDGMENTS

I want to thank Yildiz Technical University, Coordination of Scientific Research Projects for financial supporting of my project numbered 2013-01-01-GEP02.

## REFERENCES

1. Chandra, D.; Yang, S.; Lin, P. *Appl. Phys. Lett.* **2007**, *91*, 251912.
2. Jeong, H. E.; Kwak, M. K.; Suh, K. Y. *Langmuir* **2010**, *26*, 2223.
3. Menard, E.; Meitl, M. A.; Sun, Y.; Park, J.-U.; Shir, D. J. -L.; Nam, Y. -K.; Jeon, S.; Rogers, J. A. *Chem. Rev.* **2007**, *107*, 1117.
4. www.noblelight.net (Accessed February, **2014**)
5. Sperry, P. R.; Snyder, B. S.; O'Dowd, M. L.; Lesko, P. M. *Langmuir* **1994**, *10*, 2619.
6. Mackenzie, J. K.; Shuttleworth, R. *Phys. Soc.* **1949**, *62*, 838.
7. Yoo, J. N.; Sperling, L. H.; Glinka, C. J.; Klein, A. *Macromolecules* **1991**, *2424*, 2868.
8. Pekcan, Ö. *Trends Polym. Sci.* **1994**, *2*, 236.
9. Eckersley, S. T.; Rudin, A. *Prog. Org. Coat.* **1994**, *23*, 387.
10. Cannon, L. A.; Pethrick, R. A. *Macromolecules* **1999**, *32*, 7617.
11. Chevalier, Y. *Trends Polym. Sci.* **1996**, *4*, 197.
12. Pekcan, O.; Winnik, M. A.; Croucher, M. D. *Macromolecules* **1990**, *23*, 2673.
13. Ugur, S.; Elaissari, A.; Pekcan, O. *Polym. Adv. Technol.* **2005**, *16*,
14. Keddie, J. L.; Meredith, P.; Jones, R. A. L.; Donald, A. M. *Macromolecules* **1995**, *28*, 2673.
15. Arda, E.; Bulmus, V.; Piskin, E.; Pekcan, O. *J. Colloid Interface Sci.* **1999**, *213*, 160.
16. Arda, E.; Pekcan, O. *Polymer* **2001**, *42*, 7419.
17. Arda, E.; Ozer, F.; Piskin, E.; Pekcan, O. *J. Colloid Interface Sci.* **2001**, *233*, 271.
18. Pekcan, O.; Arda, E. *J. Appl. Polym. Sci.* **1998**, *70*, 339.
19. Steward, P. A.; Hearn, J.; Wilkinson, M. C. *Polym. Int.* **1995**, *38*, 23.
20. Chevalier, Y.; Pichot, C.; Graillat, C.; Joanicot, M.; Wong, K.; Maquet, J.; Lindner, P.; Cabane, B. *Colloid Polym. Sci.* **1992**, *270*, 806.
21. Schmid, A.; Sutton, L. R.; Armes, S. P.; Bain, P. S.; Manfre, G. *Soft Matter* **2009**, *5*, 407.
22. Li, F.; Winnik, M. A.; Matvienko, A.; Mandelis, A. *J. Mater. Chem.* **2007**, *17*, 4309.
23. Cingil, H. E.; Balmer, J. A.; Armes, S. P.; Pain, P. S. *Polym. Chem.* **2010**, *1*, 1323.
24. Ugur, S.; Yargi, O.; Pekcan, O. *Can. J. Phys.* **2010**, *88*, 267.
25. Arda, E.; Kara, S.; Pekcan, O. *J. Polym. Sci. Part B: Polym. Phys.* **2007**, *45*, 2918.